Communication

Improved Excitation Schemes for Multiple-Quantum Magic-Angle Spinning for Quadrupolar Nuclei Designed Using Optimal Control Theory

Thomas Vosegaard, Cindie Kehlet, Navin Khaneja, Steffen J. Glaser, and Niels Chr. Nielsen

J. Am. Chem. Soc., **2005**, 127 (40), 13768-13769• DOI: 10.1021/ja054035g • Publication Date (Web): 17 September 2005

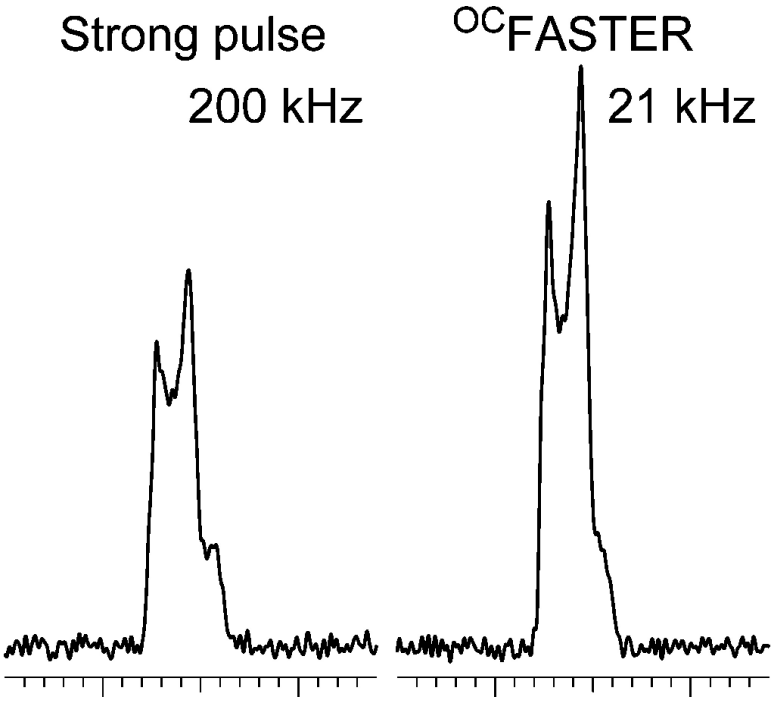

More About This Article

Additional resources and features associated with this article are available within the HTML version:

- Supporting Information
- Links to the 1 articles that cite this article, as of the time of this article download
- Access to high resolution figures
- Links to articles and content related to this article
- Copyright permission to reproduce figures and/or text from this article

View the Full Text HTML

J|A|C|S
COMMUNICATIONS

Published on Web 09/17/2005

Improved Excitation Schemes for Multiple-Quantum Magic-Angle Spinning for Quadrupolar Nuclei Designed Using Optimal Control Theory

Thomas Vosegaard,*,† Cindie Kehlet,† Navin Khaneja,‡ Steffen J. Glaser,§ and Niels Chr. Nielsen*,†

Center for Insoluble Protein Structures (inSPIN), Interdisciplinary Nanoscience Center and Department of Chemistry, University of Aarhus, DK-8000 Aarhus C, Denmark, Division of Applied Sciences, Harvard University, Cambridge, Massachusetts 02138, and Department of Chemistry, Technische Universität München, 85747 Garching, Germany

Received June 17, 2005; E-mail: tv@chem.au.dk; ncn@chem.au.dk

Optimal control (OC) theory[1] is an extremely powerful method for optimizing systems with many degrees of freedom. A host of disciplines ranging from economy to engineering has already enjoyed the benefits of OC, such as for optimizing economic investments to provide maximum outcome in a given time and under specific conditions. Addressing nuclear magnetic resonance (NMR), recent work has demonstrated the capabilities of OC to direct the nuclear spin coherences between specific initial and desired target states with improved efficiency. This has led to a variety of new liquid-state NMR experiments providing higher sensitivity or robustness toward, for example, resonance offset.[2] More recently, the underlying gradient-based OC methods[3] have been introduced to OC in solid-state NMR[4] by interfacing the OC algorithms to the SIMPSON[5] simulation software.

Bearing in mind that the power of OC is its capability to handle thousands of optimization parameters, the obvious strategy in NMR is to replace the traditional pulse sequences consisting of hard pulses and delays with much more flexible pulse waveforms for which pulse phases and amplitudes act as control variables. The result of the OC iteration is a pulse waveform containing a cascade of short pulses of variable phase and amplitude. The corresponding experiment will be carried out simply by feeding the NMR spectrometer's waveform generator with the OC pulse sequence. In solid-state NMR, the challenge is to create pulse sequences effecting the desired coherence transfer while taking into account anisotropic components of the spin interactions, sample spinning, and instrumental artifacts/limitations, such as inhomogeneity of the radio frequency (RF) fields. We note that earlier attempts to design experiments which compensate for instrumental artifacts have been based on nonlinear optimization, such as using direct spectral feedback.[6] Such approaches, however, are generally restricted to many fewer variables than the OC procedures exploited in this work.

The focus of this Communication is the widely used multiple-quantum magic-angle spinning (MQMAS) experiment.[7] This experiment offers high-resolution solid-state NMR spectra of quadrupolar nuclei with half-integer nuclear spin, normally displaying significant line broadening due to the second-order term of the quadrupole coupling interaction. The drawback of the MQMAS experiment is its low sensitivity, resulting from inefficient excitation of MQ coherences and their subsequent mixing into observable single-quantum (1Q) coherences. Since the introduction of the MQMAS experiment, a large number of studies has aimed at improving the sensitivity of the experiment by using composite or shaped pulses,[8] rotation-induced adiabatic coherence transfer (RIACT),[9] double-frequency sweeps and fast amplitude-modulated pulses,[10] rotary resonance,[11] or combinations of these[12] for the MQ excitation and MQ → 1Q mixing. Used together with rotor synchronized sampling,[13] whole-echo acquisition,[14] or QCPMG sampling,[15] significant sensitivity enhancements have been achieved during the past decade, but the low sensitivity still remains the largest problem associated with this experiment.

While the general approach has been to use the highest available RF power (desirably up to several hundred kilohertz) for the excitation and mixing pulses while keeping them short, the introduction of the more gentle FASTER (FAst Spinning gives Transfer Enhancement at Rotary resonance)[11] and to some extent RIACT[9] approaches showed that very efficient MQ excitation may be achieved in the regime of weak RF and long pulses. One drawback of the FASTER technique is that the resonance condition providing the high MQ coherences intensity is narrow, making the experiment very sensitive to RF inhomogeneity.

Nonetheless, the regime of low RF power is appealing because it dramatically relieves the requirements on the hardware and leads to less sample heating. At the same time, it is a well-suited problem for OC since long pulses allow experimental implementation of a large number of degrees of freedom in terms of RF amplitudes and phases, thereby offering the OC algorithms plenty of room to find optimum coherence transfer. Focusing on the 3Q excitation, we set up a number of OC simulations for pulse lengths of up to 5 rotor periods (τ_R) using the quadrupole coupling parameters for $RbClO_4$ ($C_Q = 3.3$ MHz, $\eta_Q = 0.2$), a spinning frequency of $\nu_R = 30$ kHz, a Larmor frequency for ^{87}Rb of 130.9 MHz (9.4 T), and a 5% Lorentzian RF inhomogeneity profile as experimental conditions.[16] Out of many results, the 5-τ_R pulse sequence shown in Figure 1a yielded the highest 3Q coherence excitation. This sequence provided a buildup of 3Q coherences, as shown in Figure 1b, where the numerical simulations are supported by experimental measurements for $^{87}RbClO_4$ using a whole-echo experiment[13] sampling only the $0 \rightarrow +3 \rightarrow +1 \rightarrow -1$ quantum coherence pathway. One very appealing feature of the sequence in Figure 1a is the low RF requirements, with a root mean square (rms) averaged RF as low as 20.7 kHz and a peak maximum of 40.5 kHz.

To evaluate the success of our new OC sequence, hereafter termed ^{OC}FASTER as it has been inspired by the FASTER excitation scheme,[11] we compared it with the standard approach using a strong (200 kHz), short (2.5 μs) excitation pulse and FASTER using a weaker (38 kHz) but longer (67 μs) pulse. The results of these comparisons are shown in Figure 1d, and the stepwise buildup of 3Q coherences as a function of the pulse length is investigated in Figure 1b. By inspection of the spectra in Figure 1d, we find that ^{OC}FASTER, for which the rms average RF power is as low as 20.7 kHz, provides a sensitivity enhancement of 41 and 45% relative to the strong-pulse and FASTER experiments,

† University of Aarhus.
‡ Harvard University.
§ Technische Universität München.

10.1021/ja054035g CCC: $30.25

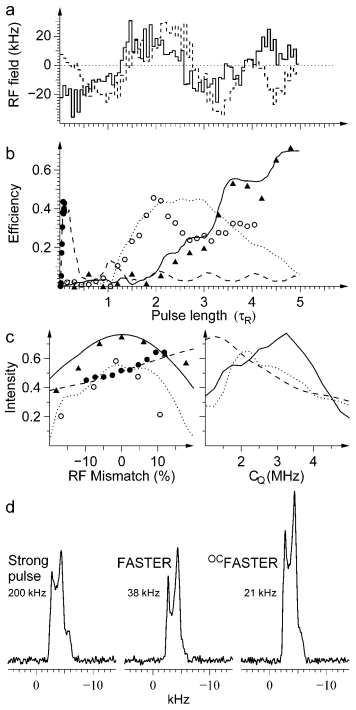

Figure 1. ^{OC}FASTER 3Q excitation for $\nu_R = 30$ kHz and $C_Q = 3.3$ MHz. (a) ^{OC}FASTER pulse sequence indicating the x (solid line) and y (dashed line) components of the RF field strength. (b) Calculated 3Q coherence buildup curves for ^{OC}FASTER (solid line), FASTER (dotted line), and strong-pulse excitation (dashed line) along with experimental measurements (^{OC}FASTER: ▲; FASTER: ○; strong-pulse: ●). (c) Stability of the three pulse sequences towards RF mismatch (left panel) and quadrupole coupling (right panel) using the same symbols as in (b). (d) Experimental 3Q filtered strong-pulse, FASTER, and ^{OC}FASTER spectra of $RbClO_4$ with indication of the average RF field strength applied. For all experiments, identical 3Q → 1Q mixing (single-pulse, 1.25 μs, 200 kHz and acquisition (whole-echo, coherent pathway: $0 \rightarrow +3 \rightarrow +1 \rightarrow -1$) conditions were applied. It should be noted that the experiments in (b) are not measured on an absolute scale, but all experimental data use the same relative scale for direct comparison of the experiments.

respectively. These numbers match well with the calculated numbers of 55 and 56% as revealed in Figure 1. In addition to this very clear improvement, the ^{OC}FASTER experiment also displays a high robustness toward RF inhomogeneity and variation in C_Q, as illustrated in Figure 1c. Although the strong-pulse experiment is less sensitive to RF variations, we note that ^{OC}FASTER has a fairly large range of high efficiency, that is, by misadjustment of the RF field strength by 10% the sequence still provides more than 85% of the optimum transfer.

The "standard" reference sample for ^{87}Rb MQMAS, $RbNO_3$, displays three sites with significantly lower C_Q's than for $RbClO_4$. On the basis of the same principles and experimental conditions as for the case of $RbClO_4$, we have designed a new ^{OC}FASTER sequence for quadrupole couplings in the regime of $C_Q = 2$ MHz. The 2D spectrum and the isotropic projection, shown in Figure 2, clearly reveal three sites, although two of them are partly overlapping at 9.4 T. Despite this, we are able to take out individual traces showing the second-order line shape for each of the three sites. Compared with a short-pulse (200 kHz, 2.5 μs) experiment, we observe significant gains on the order of 40−50% in sensitivity in favor of the ^{OC}FASTER sequence.

In conclusion, we have utilized the versatility of OC for the design of MQMAS experiments for quadrupolar nuclei and demonstrated this by specific pulse sequences that improve the sensitivity by about 50%, which is a very significant improvement relative to earlier approaches.

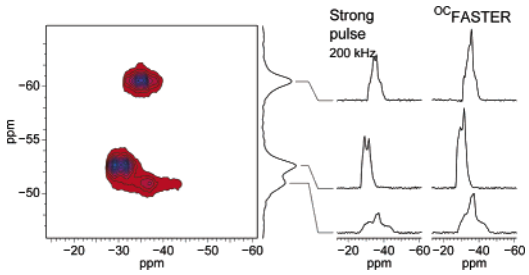

Figure 2. Two-dimensional ^{87}Rb MQMAS experiment of $RbNO_3$ at 9.4 T. The 2D spectrum on the left and the vertical projection of the isotropic dimension reveal the three Rb sites. The traces showing the second-order line shapes on the right show characteristic and well-resolved second-order quadrupolar line shapes for each site. Traces are shown for the spectrum recorded using short-pulse excitation using 200 kHz RF field strength, and ^{OC}FASTER excitation are shown in the left and right panels, respectively. The mixing and acquisition protocols are identical to those reported in Figure 1.

Acknowledgment. Support from the Danish National Research Foundation, the Danish Natural Science Research Council, Carlsbergfondet, and the Danish Biotechnology Instrument Centre is acknowledged. S.J.G. acknowledges financial support from DFG Grant Gl 203/4-2.

Supporting Information Available: The pulse sequence waveforms applied for the experiments on $RbClO_4$ and $RbNO_3$. This material is available free of charge via the Internet at http://pubs.acs.org.

References

(1) (a) Pontryagin, L.; Boltyanskii, B.; Gamkreldze, R.; Mishchenko, E. *The Mathematical Theory of Optimal Processes*; Wiley-Interscience: New York, 1962. (b) Bryson, A., Jr.; Ho, Y.-C. *Applied Optimal Control*; Hemisphere: Washington, DC, 1975.
(2) (a) Khaneja, N.; Luy, B.; Glaser, S. J. *Proc. Natl. Acad. Sci. U.S.A.* **2003**, *100*, 13162. (b) Khaneja, N.; Li, J.-S.; Kehlet, C.; Luy, B.; Glaser, S. J. *Proc. Natl. Acad. Sci. U.S.A.* **2004**, *101*, 14742. (c) Kobzar, K.; Skinner, T. E.; Khaneja, N.; Glaser, S. J. *J. Magn. Reson.* **2004**, *170*, 236.
(3) Khaneja, N.; Reiss, T.; Kehlet, C.; Schulte-Herbrüggen, T.; Glaser, S. J. *J. Magn. Reson.* **2005**, *172*, 296.
(4) (a) Kehlet, C. T.; Sivertsen, A. C.; Bjerring, M.; Reiss, T. O.; Khaneja, N.; Glaser, S. J.; Nielsen, N. C. *J. Am. Chem. Soc.* **2004**, *126*, 10202. (b) Kehlet, C. T.; Vosegaard, T.; Khaneja, N.; Glaser, S. J.; Nielsen, N. C. *Chem. Phys. Lett.*, in press.
(5) Bak, M.; Rasmussen, J. T.; Nielsen, N. C. *J. Magn. Reson.* **2000**, *147*, 296. Open source software, web-site: http://www.bionmr.chem.au.dk.
(6) de Paëpe, G.; Hodgkinson, P.; Emsley, L. *Chem. Phys. Lett.* **2003**, *376*, 259.
(7) Frydman, L.; Harwood, J. S. *J. Am. Chem. Soc.* **1995**, *117*, 5367.
(8) (a) Ding, S.; McDowell, C. A. *Chem. Phys. Lett.* **1997**, *275*, 188. (b) Marinelli, L.; Medek, A.; Frydman, L. *J. Magn. Reson.* **1998**, *132*, 88.
(9) Wu, G.; Rovnyak, D.; Sun, B.; Griffin, R. G. *Chem. Phys. Lett.* **1996**, *249*, 210.
(10) (a) Kentgens, A. P. M.; Verhagen, R. *Chem. Phys. Lett.* **1999**, *300*, 435. (b) Madhu, P. K.; Goldbourt, A.; Frydman, L.; Vega, S. *Chem. Phys. Lett.* **1999**, *307*, 41.
(11) Vosegaard, T.; Florian, P.; Massiot, D.; Grandinetti, P. J. *J. Chem. Phys.* **2001**, *114*, 4618.
(12) (a) Madhu, P. K.; Levitt, M. H. *J. Magn. Reson.* **2002**, *155*, 150. (b) Siegel, R.; Nakashima, T. T.; Wasylishen, R. E. *Chem. Phys. Lett.* **2005**, *403*, 353.
(13) Massiot, D. *J. Magn. Reson. A* **1996**, *122*, 240.
(14) (a) Massiot, D.; Touzo, B.; Trumeau, D.; Coutures, J. P.; Virlet, J.; Florian, P.; Grandinetti, P. J. *Solid State Nucl. Magn. Reson.* **1996**, *6*, 73. (b) Brown, S. P.; Wimperis, S. *J. Magn. Reson.* **1997**, *124*, 279. (c) Vosegaard, T.; Florian, P.; Grandinetti, P. J.; Massiot, D. *J. Magn. Reson.* **2000**, *143*, 217.
(15) (a) Vosegaard, T.; Larsen, F. H.; Jakobsen, H. J.; Ellis, P. D.; Nielsen, N. C. *J. Am. Chem. Soc.* **1997**, *119*, 9055. (b) Larsen, F. H.; Nielsen, N. C. *J. Phys. Chem. A* **1999**, *103*, 10825.
(16) The chosen RF profile matches the profile of a 4 mm Bruker MAS probe and a 9.2% Gaussian inhomogeneity.

JA054035G